Removal of Aqueous Copper(II) by Using Crosslinked Chitosan Films

Jéssica S. Marques[1,2], Márcia R. Pereira[1], Arcadio Sotto[2], Jesús M. Arsuaga[2,*]

[1]Chemistry Institute, Universidade Federal do Rio Grande do Norte, Campus Universitário, Lagoa Nova, Natal, RN 59072-970, Brazil

[2]School of Experimental Science and Technology, ESCET, Rey Juan Carlos University, 28933-Móstoles, Madrid, Spain.

*Corresponding author: jesusmaria.arsuaga@urjc.es

Graphical abstract

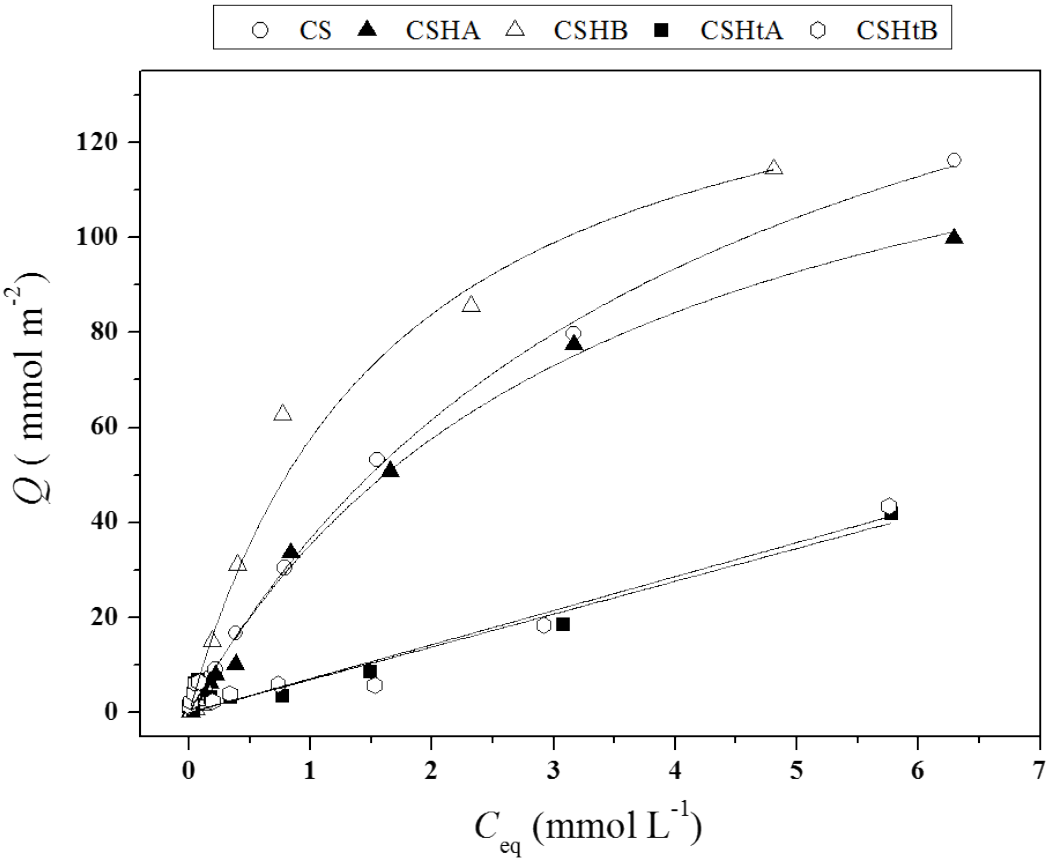

Synopsis: Chitosan, a cheap product obtained from chitin, is modified and manufactured as films for treating water streams containing copper.

Abstract:

Chitosan films crosslinked with sulfuric acid were prepared by using two different methodologies named as homogeneous and heterogeneous. The Cu(II) adsorption capacity of the films was studied by means of kinetic and equilibrium experiments. Neat chitosan (CS) and homogeneously crosslinked samples (CSHA and CSHB) exhibited quite similar performances for aqueous Cu^{2+} removal (near to 80% for 14 ppm aqueous solutions); whereas the adsorption capacity of heterogeneous films (CSHtA and CSHtB) was significantly lower. The pseudo-second order model adequately reproduced the kinetics curves, while the Freundlich isotherm was preferable for modelling the equilibrium. The capability of the chitosan films for pressure-driven filtration of water solutions was explored by determining pure water permeability along with the flux and rejection of aqueous Cu^{2+} solutions. Water flux was thoroughly low in the order: CSHA ≥ CS >> CSHtA. The permeate flux observed for modified chitosan membranes during filtration experiments with aqueous Cu(II) solutions was steady, being significantly higher for the homogeneous samples. All the prepared films exhibited excellent antifouling properties and the crosslinked specimens also enhanced Cu^{2+} rejection potential (above 95%). The homogeneously crosslinked film CSHA appeared as a promising material for the treatment by adsorption and filtration of aqueous copper streams.

Keywords: Chitin; sulfuric acid crosslinking; metal adsorption; permeability; copper rejection; water treatment.

1. Introduction

Chitin is usually considered the second polysaccharide most abundant in nature after cellulose, being the main structural component of crustaceans, insects, and fungi. Chitosan is produced from the *N*-deacetylation of chitin which is obtained primarily from selfish waste as a by-product of seafood industry [1]. Despite its huge annual production and easy availability, chitin still remains an under-utilized resource mainly because of its rather rigid molecular structure [2,3]. However, when chitin is deacetylated above 50%, it turns soluble in acidic solutions and becomes chitosan, a very compatible and effective biomaterial to be used in many applications [4,5]. Chitosan is a polysaccharide copolymer formed of 2-acetamido-2-deoxy-*D*-glucopyranose and 2-amino-2-deoxy-*D*-glucopyranose with structure similar to cellulose, where amino groups (mostly) and acetamido groups (rarely) are anchored instead of the hydroxyl groups on the carbon-2 of the cellulose-like backbone as seen in Fig. 1S. Due to the presence of reactive amino and hydroxyl groups into its chemical structure, chitosan forms water insoluble complexes with anionic polyelectrolytes and chelates metal ions [6]. Chitosan can be readily prepared under a wide variety of forms such as fibers, powder, micro and nanoparticles, beads, and films, among others [7–10].

The removal of ionic pollutants like heavy metals from water streams could become an important application of chitosan films used as sorbents and/or filters. However, the free amino groups ($–NH_2$) present in each monomeric unit of chitosan are readily protonated to alkyl ammonium cations ($-NH_3^+$) in aqueous acidic media. Hence, chitosan films are easily dissolved or converted into gels depending on the solution pH value, the polymeric chains molecular weight, and the deacetylation degree. Crosslinking is an adequate chemical route to make chitosan almost insoluble through the interactions between adjacent polymer chains that promote the formation of a restricted network. In addition, crosslinking also improves the thermal, chemical, and mechanical resistance of chitosan films which can attain the necessary stability for use in water treatment technology [11].

The diversity of tested crosslinking agents is very wide including glutaraldehyde [7], epichlorohydrin [8], genipin [9], tripolyphosphate [10], and sulfuric acid [12]. Some crosslinkers as glutaraldehyde connect chemically, *i.e.* by covalent bonds, the adjacent polymer chains, whereas other crosslinking agents, as phosphoric and sulfuric acids, mainly

act through an ionic mechanism. Particularly, the properties of chitosan films crosslinked with sulfuric acid are of increasing interest in filtration technology; thus, for water mixtures a higher separation factor along with less permeation flux has been reported [12]. The crosslinking process ordinarily occurs heterogeneously, where pure chitosan films are immersed in a sulfuric acid solution. However, the alternative one-step synthesis route, termed as homogenous, has received much less attention [13]. Therefore, both crosslinking routes are analyzed and compared in this work that is focused to the preparation of chitosan films intended for aqueous metal removal.

Numerous studies have demonstrated the effectiveness of chitosan and modified products to recovery heavy metals from water solutions [14-16]. Heavy metals exhibit high levels of toxicity and poor degradability; consequently, they are a serious environmental concern promoted by agricultural waste, that includes fertilizers and fungicides, along with industrial residues, paints, pigments, batteries, and urban wastewater [17]. Among them, copper(II) is a toxic metal that at high concentrations can generate adverse effects to the human health [18]. In this context, chitosan films appear as an alternative for the recovery of copper ions from water solutions, due to their hydrophilicity, determined by the presence of hydroxyl and amino groups, high reactivity of these organic functionalities ($–NH_2$ and –OH), and flexible structure of the polymer chains [6,18]. The use of this type of films, frequently integrated into multilayer or composite membranes, can be an advantageous separation tool against other alternative methods due to the availability of the starting material, its non-polluting nature, and energy saving process [19–21].

For the chemical structure and mechanical properties of the synthetized crosslinked chitosan films was previously reported [13], the present investigation was devoted to determine their sorption and transport properties for aqueous solutions containing Cu^{2+} salts. Metal adsorption capacity, water permeation flux, and salt retention were specifically evaluated.

2. Material and methods

2.1 Materials

Chitosan was obtained from Sigma–Aldrich (Germany) with low molecular weight (LMW) and deacetylation degree of 75–85%. Acetic acid (P.A. 99.5%, Scharlau S.L., Spain), hydroxide sodium (NaOH P.A. 97%, Scharlau S.L., Spain), sulfuric acid (H_2SO_4, P.A. 95–97%, Sigma–Aldrich, Germany), and copper (II) sulfate-pentahydrate ($CuSO_4 \cdot 5H_2O$ 98%, Sigma–Aldrich, Germany) were used without further purification.

2.2 Preparation and chemical modification of chitosan films

Neat and crosslinked chitosan films were prepared as previously reported [13,22]. Hence, just a short recapitulation is shown here. Two types of crosslinking procedures were accomplished: homogeneous (H) and heterogeneous (Ht). Homogeneous crosslinking process was carried out by the addition of H_2SO_4 solution (0.5 M) to the chitosan solution with two different SO_4^{2-}/NH_3^+ ratios under mechanical agitation for 1 h at room temperature [13]. Subsequently, solvent evaporation, neutralization, and dry processes were completed in the same conditions of neat chitosan films preparation. Heterogeneous crosslinking process was performed by immersing the neat chitosan films, after the neutralization process, into a H_2SO_4 solution (0.5 M) during two different time intervals; then, films were washed with distilled water and dried [13]. The internal modification provoked in the chitosan structure by the crosslinking process with sulfuric acid can be visualized in Fig. 2S. Accordingly, five different chitosan films were obtained: neat chitosan (CS), homogeneously crosslinked chitosan (CSHA and CSHB), and heterogeneously crosslinked chitosan (CSHtA and CSHtB). The nomenclature and composition of the prepared materials are listed in Table 1, where experimental water contact angle at the film surface is also included.

Table 1.
Composition of the casting solutions and experimental water contact angles of prepared films.

Material	Ratio SO_4^{2-}/NH_3^+	Immersion time (min)	Contact angle (°)
CS	–	–	88.2
CSHA	1 : 6	–	88.6
CSHB	1 : 4	–	90.3
CSHtA	–	5	96.4
CSHtB	–	30	95.1

Film characterization

Prepared films were chemically characterized by using Varian 3100 FTIR ATR between 6000 and 400 cm^{-1} and 64 scans. Surface hydrophilicity was evaluated through water contact angles determined by Drop Shape Analysis System using a KSV CAM 200 instrument operated in static mode (KSV instruments, USA).

2.3 Adsorption experiments

Copper adsorption experiments were accomplished inside closed stainless steel containers where the salt solution was brought in contact exclusively with the upper film layer. The experimental equipment is shown in Figure 3S. All of the essays were thermostatically controlled at 15 or 30 °C under constant magnetic stirring (300 rpm). The solution volume (V) was 150 mL and the effective area of the samples (A) was 20 cm^2. Blank experiments were carried out to determine the effect of water evaporation and solute adsorption onto the recipient walls [23].

The amount of ionic metal adsorbed was calculated by Eq. (1):

$$Q = \left[\left(\frac{(C_i - C_{eq}) - (C_i - C_b)}{A} \right) \times V \right] \quad (1)$$

where C_i, C_b, and C_{eq} are the initial, blank, and equilibrium concentrations of aqueous Cu(II) solutions, respectively. Inductively coupled plasma atomic emission spectroscopy (ICP-AES, model Varian 720-ES) was thoroughly used in this work to determine metal concentrations, both in sorption and filtration experiments.

2.3.1 Adsorption kinetics

The kinetics study provides valuable information about adsorption mechanisms which involve mass transfer, diffusion, and surface reaction during the sorption process [24]. In order determine the kinetic mechanism for the adsorption of Cu^{2+} on the chitosan films, the contact between the stirred feed solution and the upper layer of the sample was controlled during seven time intervals (0.5, 1, 3, 6, 15, 24, and 48 h). The initial concentration of metal solution was fixed at 14 ppm at 30 °C, and 100 ppm at 15 and 30 °C. Semiempirical pseudo-

first order and pseudo-second order kinetic models were fitted to the experimental data according their integrated forms, Eq. (2) and Eq. (3), respectively:

$$q_t = q_e\left[1 - \exp(-k_1 t)\right] \quad (2)$$

$$\frac{t}{q_t} = \frac{1}{k_2 q_e^2} + \frac{t}{q_e} \quad (3)$$

where q_e and q_t are the copper amounts (mmol m^{-2}) adsorbed at equilibrium and time t (h), respectively, k_1 is the pseudo-first order adsorption rate constant (h^{-1}), and k_2 is the pseudo-second order kinetic constant ($mmol^{-1}$ m^2 h^{-1}). Likewise, the validity of the intra-particle diffusion model validity was tested for the sorption process under study by means of Eq. (4):

$$q_t = k_{id}\sqrt{t} + C \quad (4)$$

where k_{id} is the intra-particle diffusion rate constant and C, the intercept of the plot, is related to the thickness of the boundary layer [24,25].

2.3.2 Adsorption isotherms

The Langmuir and Freundlich adsorption isotherms were used to describe the adsorption of Cu^{2+} ions on the films. The Langmuir model assumes that all sites adsorb to the same extent and predicts the formation of an adsorbate monolayer on the sorbent surface [26], whereas the Freundlich model supposes that the adsorbent has a heterogeneous surface with an exponential energetic distribution of the different adsorption sites [23]. Thus, experimental data were analyzed by means of the Langmuir and Freundlich adsorption isotherms represented by Eq. (5) and (6), respectively:

$$Q = \frac{Q_{\max} k_L C_{eq}}{1 + k_L C_{eq}} \quad (5)$$

$$Q = k_F C_{eq}^n \quad (6)$$

where Q is the quantity adsorbed at equilibrium on solid phase, $Q_{\max}$ is the maximum amount adsorbed on a monolayer, k_L is the Langmuir constant, which is related to adsorption energy, C_{eq} is the equilibrium concentration in the solution phase, and k_F and n are the Freundlich isotherm constants indicating the adsorption capacity and adsorption intensity, respectively.

2.4 Pressure-driven filtration experiments

The manufactured films were characterized in terms of water flux using a cross-flow filtration configuration. The filtration system used in this study was the same as described elsewhere and shown in Figure 4S. [27]. The equipment was operated in a recycle mode to achieve a constant feed composition and the temperature was controlled at 25.0 ± 0.1 °C by means of a thermostatic bath. The operation pressure (Δp) was varied within 2–15 bar for the neat sample (CS) and 15–25 bar for the modified specimens (CSH and CSHt). The permeability was determined as the slope of the water flux/pressure plot in the linear interval.

Chitosan films were soaked in distilled water for 24 h in order to explore its swelling capacity. After that, the samples were compacted inside the cross-flow permeation cell with distilled water during 1h at 15 bar for CS and at 25 bar for CSH and CSHt films. Water permeate flux (J_w) was determined from the amount of permeate collected during 2 min by using an analytical balance.

Copper salt solutions were recirculated to evaluate the permeation performance of chitosan films. The concentration of the Cu(II) feed solution was fixed at 14 ppm. Permeate, feed, and concentrate aliquots were collected every hour in the course of the whole experiment carried out at Δp = 15 bar. The Cu^{2+} ions rejection R was calculated by Eq. (7):

$$R(\%) = \left(1 - \frac{C_p}{C_f}\right) \times 100 \tag{7}$$

where C_p and C_f are the permeate and feed concentrations, respectively.

To estimate the fouling extent, the tested films were cleaned with fresh water inside the filtration cell after the copper sulfate permeation experiments. Then, the irreversible fouling of the materials was estimated as the pure water flux ratio after (J_{wf}) and before (J_{wi}) salt filtration. In addition, the flux decline promoted by the salt solution was determined in terms of relative flux (RF) by Eq. (8):

$$RF = \left(\frac{J_{Cu}}{J_{wi}}\right) \tag{8}$$

where J_{Cu} is the copper solution flux.

3. Results and discussion

3.1 Characterization of the chitosan films

The chemical structure, stability in acidic solution, mechanical parameters, and textural properties of the prepared materials were previously described in detail and only significant features will be mentioned here [13]. The first and simplest distinction that is possible to appreciate between the different films is associated to their color. Whereas CS, CSHtA, and CSHtB specimens showed brown light appearance, CSHA and CSHB films exhibited yellow light color. Likewise, the thickness of chitosan films enlarged from 50 to 70 μm as result of the crosslinking process as summarized in Table 1S. In addition, crosslinked samples became less hydrophilic due to the loss of amino binding sites ensued during the reaction with H_2SO_4 [28]. Figure 5S shows the FTIR-ATR spectra of neat chitosan and crosslinking specimens that were similar to the found in literature. A detailed analysis of these FTIR-ATR spectra was already reported [13].

As previously described, the neat chitosan films exhibited a very flexible and ductile consistency rather inadequate for working under pressure. However, that changed to a more rigid configuration with the addition of the crosslinking agent due to the formation of three-dimensional networks [13,30]. Therefore, more compact structures with less flexible polymer chains were generated as result of the crosslinking density increase [31,32].

In addition, the hydrophilicity of the prepared films was evaluated through water contact angle experiments. Fig. 1 shows some images of water drops deposited on CS, CSHA, and CSHtA films. As seen in Table 1, that summarizes the values obtained for every specimen as the mean of four runs, the hydrophilicity increased in the order: CSHtB ≈ CSHtA < CSHB < CSHA ≈ CS. Water affinity would facilitate the ions diffusion through the films due the mobility of H_2O molecules in such system [33,34]. The poorer wettability of the CSHtA and CSHtB samples should be related with the textural alteration occurred during the film formation. In effect, since these films were prepared through the immersion of neat chitosan samples in the H_2SO_4 solution, the amino groups at the film surface were considerably affected leading to the blockage of water crossing. Furthermore, it has been reported elsewhere that heterogeneous crosslinking procedure using sulfuric acid modifies the heterogeneity of the outer surface of chitosan films promoting a more dense and smooth surface [11]. Conversely, homogeneous crosslinking was carried out within the casting

solution and using lower amounts of sulfuric acid; thus, this procedure preserved numerous free amino groups both superficially and inside the film bulk.

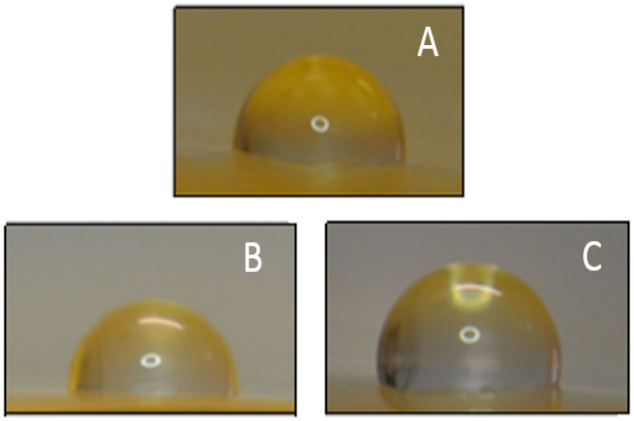

Fig. 1. Water contact angle images of CS (A), CSHA (B), and CSHtA (C) films

3.2 Copper adsorption experiments

The capacity of adsorption of the prepared chitosan films was assessed through kinetic and equilibrium experiments. According to the subsequent filtration study, the initial copper concentration was selected at 14 ppm that is close but higher than the copper discharge limit (<1.00 ppm). Temperature was regulated at 30 ºC, very similar to the temperature in the filtration investigation. However, in order to complete the kinetic adsorption study, an initial Cu(II) concentration of 100 ppm was also evaluated. This concentration, usually found in literature, corresponds to copper polluted wastewater. In addition, some kinetic experiments were carried out at 15 ºC to test the effect of temperature on adsorption.

Firstly, some preliminary adsorption experiments were accomplished with aqueous Cu(II) solutions (14 and 100 ppm) as described in section 2.4 in order to explore the copper uptake capacity of the prepared chitosan films. The values obtained at equilibrium are shown in Table 2, where it is apparent that, after contact during 48 h, neat and homogeneously chitosan films show significant capacity for copper ions removal. It is remarkable that the CSHA sample exhibited a Cu(II) adsorption capacity higher than the neat CS film. Conversely, the heterogeneous crosslinking procedure drastically reduced the adsorption of Cu^{2+} ions. These promising preliminary experiments encouraged the subsequent adsorption study.

Table 2.
Removal of aqueous Cu^{2+} attained with the prepared films after contact during 48 h.

Film	Percent removal (%)		
	14 ppm (30 °C)	100 ppm (30 °C)	100 ppm (15 °C)
CS	73	42	46
CSHA	80	53	59
CSHB	73	54	38
CSHtA	14	22	9
CSHtB	13	2	4

3.2.1 Adsorption kinetics study

The Figs. 2(A) and 2(B) show the temporal evolution of metal ion adsorption curves obtained for chitosan films at 30 ºC for two different initial metal concentrations (14 and 100 ppm). Firstly, the experiments were accomplished using more dilute solutions (14 ppm), according to copper content observed in the industrial wastewater streams (Fig. 2A). Under this experimental conditions (low metal content), neat and homogeneous samples exhibited higher adsorption capacity (around 70% of initial content) as compared to heterogeneous specimens.

The rather similar behavior observed for CS, CSHA, and CSHB materials suggests that the number of available $–NH_2$ groups on the film surface interacting with metal ions is hardly affected by the homogeneous crosslinking procedure. The fair agreement observed for CS and CSH films in both adsorption kinetics and water contact angle reveals that hydrophilicity is a favorable factor for copper adsorption. In the opposite, CSHtA and CSHtB films saturated at very low metal content in the first 10 h of contact time.

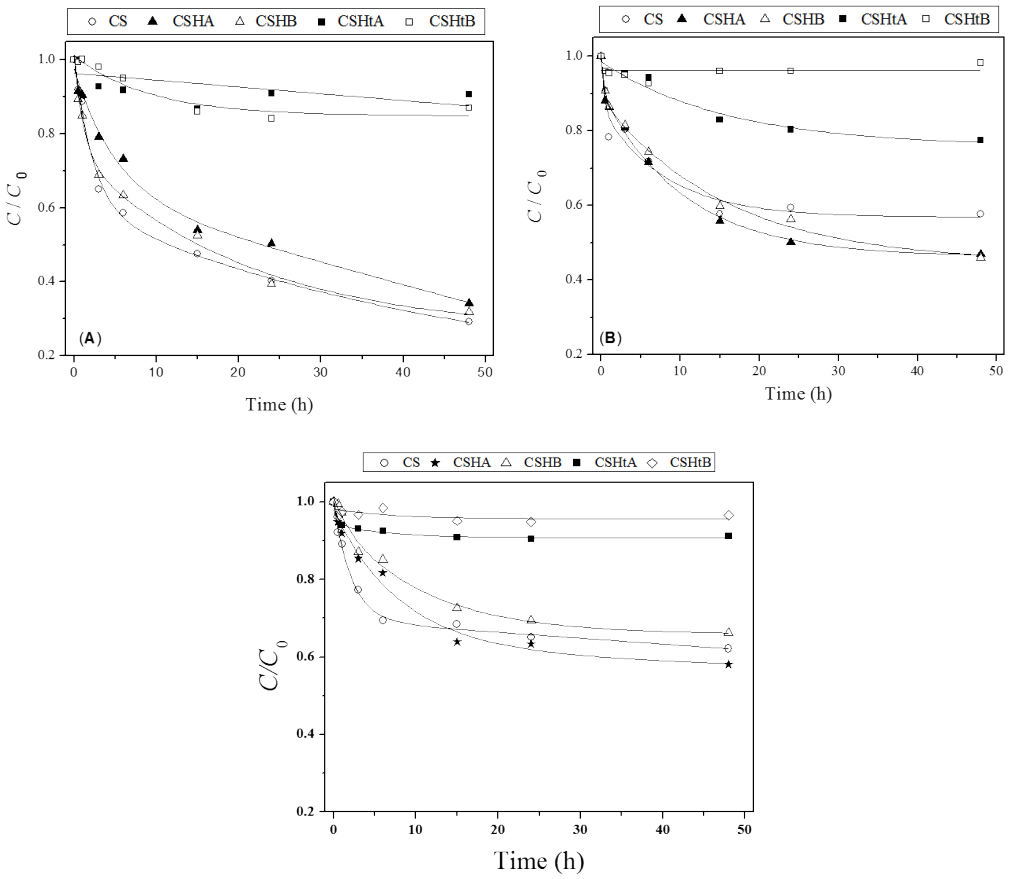

Fig. 2. Adsorption kinetics of Cu^{2+} on chitosan films.
(A) 14 ppm and 30 °C.
(B) 100 ppm and 30 °C.
(C) 100 ppm and 15 °C.

The increase of initial metal concentration up to 100 ppm (Fig. 2B) enhances the diffusive drive force that promotes the adsorption phenomenon. The salt content is proportional to the probability that the ion-NH_2 group interaction will occur. It is apparent that saturation state was systematically reached at 48 h when 100 ppm copper solutions were evaluated. For this experimental conditions, both homogeneous crosslinking films (CSHA and CSHB) exhibited the highest values of Cu(II) adsorption, similar (or surpassing) to the capacity of the neat chitosan sample. The two heterogeneous films showed a rather distinct adsorption extent not observed at 14 ppm with a difference between them near 20%. The presence of residual active sites on the CSHtA surface (prepared with only 5 minutes of crosslinking reaction) makes possible some ion adsorption when Cu(II) concentration rises up to 100 ppm.

The influence of temperature on the adsorption process was tested through additional experiments carried out at 15 °C and 100 ppm of metal concentration (Fig. 2C). In general, the adsorption extent was slightly reduced when the temperature decreased. Besides, the difference between CSHtA and CSHtB samples diminished to 5 %. The reduction of adsorption capacity when temperature lowered indicates that sorption behaves as a endothermic process, although the effect could be also attributed to structural changes in the films surface due to the restriction of chitosan chains mobility [35].

The kinetics results were compared with the predictions of the two usual global models, pseudo-first and pseudo-second order. The fitting parameters are summarized in Table 3. For purposes of comparison, the experimental q_e values determined at 48 h are also summarized in Table 2S. As it can be inferred from R^2, the pseudo-second order model is preferable and acceptably reproduces the experimental data. It is possible to observe a slight increase in q_e for the homogeneous crosslinking chitosan films in comparison with neat chitosan, although the kinetics for the CS, CSHA, and CSHB is quite similar in the experimental conditions.

The kinetics of the Cu(II) adsorption on chitosan films was evaluated at the natural pH of the copper sulfate aqueous solutions. pH was not adjusted to reduce the medium alteration and simultaneously prevent the precipitation of copper hydroxide occurring when pH is above 6. Likewise, there are some clear evidences revealing that chitosan materials exhibit the greatest metal uptake within pH 4–6. However, at very acidic pH, the amino groups of chitosan would be intensely protonated and the resultant NH^{3+} groups would produce electrostatic repulsion between the adsorbent surface and the positively charged copper species impeding adsorption. The mechanism of the studied adsorption process is commonly assumed to occur through chelation of copper ions with $–NH_2$ and –OH groups of chitosan. Thus, Domard suggested the formation of a tetradentate structure $[CuNH_2(OH)_2]$ [36]. Although other authors indicated that acidification should promote a chemical competition between copper-amino chelation and protonation of amino groups from chitosan ($–NH_2$ to $–NH_3^+$) [37–39].

In the present study, where solution pH was around 5.3 for kinetics experiments, copper chelation with hydroxyl and amino groups was not lower for CSH films than for the neat chitosan specimen, because the homogeneous crosslinking process hardly affected the amino groups at the surface films. Conversely, the poor sorption capacity that heterogeneous

material exhibited, as revealed by the low q_e values determined for CSHtA and CSHtB, can be explained taking into account that these samples were prepared by immersion of neat chitosan films in strong acid media. Therefore, the external surface amino groups were preferentially crosslinked and the removal of aqueous Cu^{2+} ions was prevented by the absence of available $–NH_2$ free groups.

Table 3.
Kinetics parameters for the adsorption of Cu^{2+} ions by chitosan films.

		Pseudo-first-order			***Pseudo-second-order***		
		q_e (mmol m^2)	k_1 (h^{-1})	R^2	q_e (mmol m^2)	k_2 (h^{-1})	R^2
Adsorption of Cu^{2+} ions at 30 °C (14 ppm)	CS neat	12.0	0.123	0.937	12.8	0.017	0.994
	CSHA	10.1	0.109	0.961	11.0	0.015	0.989
	CSHB	12.0	0.097	0.986	12.4	0.023	0.991
	CSHtA	2.5	0.109	0.310	2.59	0.336	0.974
	CSHtB	2.7	0.114	0.795	4.04	0.013	0.887
Adsorption of Cu^{2+} ions at 30 °C (100 ppm)	CS neat	51.7	0.139	0.983	53.5	0.010	0.999
	CSHA	64.5	0.134	0.978	69.4	0.004	0.992
	CSHB	65.5	0.125	0.922	69.9	0.003	0.985
	CSHtA	28.0	0.108	0.973	32.5	0.004	0.904
	CSHtB	7.2	0.0.4	0.148	5.81	0.666	0.999
Adsorption of Cu^{2+} ions at 15 °C (100 ppm)	CS neat	50.0	0.145	0.868	53.1	0.009	0.981
	CSHA	58.0	0.079	0.969	62.6	0.002	0.989
	CSHB	43.5	0.090	0.994	51.3	0.002	0.976
	CSHtA	12.9	0.106	0.737	12.8	0.256	0.999
	CSHtB	5.5	0.009	0.416	5.40	0.249	0.998

Along with the pseudo-first and pseudo-second order kinetic models, the adequacy of the intra-particle diffusion model for interpreting the kinetics of the copper adsorption was evaluated through Eq. 4 [24]. The fitting kinetic constants, k_{id}, and regression factors, R^2, estimated for prepared materials are listed on Table 4. In all cases, the fitting is poorer than obtained from the pseudo-second order model. Besides, the heterogeneous chitosan films, CSHtA and CSHtB, exhibited the lowest intra-particle diffusion rates. This effect is coherent

with pseudo-second order model assumption that describes the adsorption performance in terms of superficial layer formation. CSHA and CSHB showed better correlation coefficients for both 14 and 100 ppm initial concentration at 30 °C. The increase of the Cu^{2+} ions concentration enhanced the diffusion of ions to the inner film layer rising the rate constants from 1.4 to 8.7, approximately. The comparison between experimental results at 30 ºC and 15 ºC demonstrated that diffusion was favored at lower temperature for CS, CSHA, and CSHB films, while no conclusion could be extracted for CSHtA and CSHtB samples due to the inadequacy of the fitting.

Table 4.
Parameters kinetics of diffusion intra-particle for the adsorption of Cu^{2+} ions by chitosan films.

Film	Adsorption Cu^{2+} ions					
	14 ppm (30°C)		100 ppm (30°C)		100 ppm (15°C)	
	k_{id}	R^2	k_{id}	R^2	k_{id}	R^2
CS neat	1.62	0.899	5.56	0.837	6.61	0.903
CSHA	1.45	0.954	8.63	0.942	11.35	0.916
CSHB	1.42	0.946	8.76	0.972	6.69	0.908
CSHtA	0.35	0.443	4.16	0.872	0.525	0.684
CSHtB	0.49	0.877	-0.11	0.238	0.362	0.611

3.2.2 Equilibrium isotherms of Cu(II) adsorption

The equilibrium results of aqueous Cu^{2+} adsorption on chitosan films at 30 ºC are shown as isotherms in Figure 3, where the adsorbed amount (Q, mmol m^{-2}) is plotted vs equilibrium concentration (C_{eq}, mmol L^{-1}). Most experimental values were collected at low metal concentration according to the previous kinetic study (C_{eq} < 30 ppm or 0.5 mmol L^{-1}). However, in order to distinguish better the sorption performance of each selected chitosan film, the concentration range was extended with additional experiments up to C_{eq} = 6 mmol L^{-1} (400 ppm). The precipitation of copper hydroxide was prevented by the natural pH of the Cu(II) solutions, clearly below 5. Nevertheless, despite this enlarged concentration study, saturation of chitosan films was reached in no case. Neat chitosan and homogenous specimens exhibited rather similar isotherms, while the adsorption performance of the two heterogeneous films was identical with sorption capacities much lower than found for CS, CSHA, and CSHB.

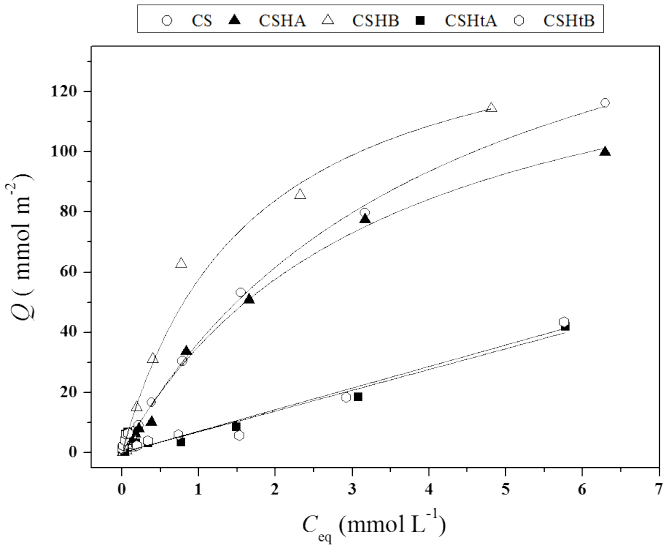

Fig.3. Adsorption equilibrium isotherms of Cu^{2+} ions on chitosan films at 30 °C.

The fitting of the Langmuir and Freundlich models to experimental isotherms was accomplished and the obtained parameters summarized in Table 5. The predictions of the Freundlich model were thoroughly superior, save for CSHB membrane. It is remarkable, as mentioned above, that the sorption saturation of the films was not attained in any case, in spite of the high initial copper concentration studied. Perhaps, this fact could be attributed to the experimental procedure where the membrane samples were not immersed into the salt solution, so reducing the effective sorption area.

Table 5. Adsorption isotherm parameters for adsorption of Cu^{2+} ions by chitosan films.

	Langmuir			**Freundlich**		
	Q_{max} (mmol m^2)	b	R^2	k_F	n	R^2
CS neat	178.6	0.277	0.894	31.66	0.793	0.988
CSHA	172.4	0.233	0.867	28.05	0.849	0.986
CSHB	147.1	0.687	0.983	41.80	1.429	0.911
CSHtA	46.7	0.310	0.243	8.77	0.411	0.537
CSHtB	39.06	0.481	0.299	9.72	0.340	0.673

Several studies explained that amine sites are reactive groups for metal adsorption, though hydroxyl groups in the C-3 position may also contribute to sorption. The adsorption

process is expected to occur in two stages. Firstly, it takes place the mass transfer of Cu^{2+} ions to the film surface [42] and, then, the subsequent metallic ions diffusion inside the film where free $–NH_2$ groups remain available for Cu^{2+} interaction. Therefore, the deep modification of the membrane surface produced by the heterogeneous crosslinking inhibits the adsorption process. This effect could also determine the water permeation of heterogeneous chitosan films during filtration experiments. Finally, it should be emphasized the difficulty of relating the copper adsorption values obtained in this work with other studies, because adsorption experiments are usually carried out by dipping some pieces of the films into the metal solution, whereas in this study the copper solution is only in contact with one surface of the films, as required for subsequent filtration tests.

3.3 Filtration experiments

3.3.1 Water flux experiments

Neat chitosan films (CS) behave as dense films. Some swelling studies reported that water diffusion into the chitosan is promoted due to its hydrophilic character [43]. Sulfuric acid is a binary crosslinking agent that reacts through the ionic interactions with $-NH_3^+$ reducing the $–NH_2$ groups content which can be responsible of the hydrophilicity decrease on the film surface. This effect was confirmed by the contact angle experiments summarized in Table 1. Previous studies of crosslinked films showed a similar decrease in the hydrophilic behavior [44].

Fig. 4 shows the evolution of pure water permeate flux with applied pressure. As seen from the figure, CS film exhibits some permeate water flux even at low pressure, which indicates that the free mobility of polymer chains promotes the formation of higher internal free volume. Thus, the water molecules access to the inner structure of the film enabling water transport at low pressure. Although, according to its permeation range, CS films should be classified as nanofiltration membranes with water permeability as low as shown in Table 6. This assessment is consistent with its ability for divalent ions rejection.

In general, crosslinking modified films exhibit lower permeation capacity than neat CS sample, since the crosslinking process causes an adverse impact on the swelling capacity [43]. However, the permeability of the two evaluated homogeneous modified materials, CSHA and CSHB, was rather similar to that of CS and significant differences between them were only observed at pressure values over 20 bar.

Taking into account the identical adsorption performances observed for both heterogeneous samples prepared in this study, only one of them, namely CSHtA, was selected for further investigation on filtration. This heterogeneous film showed the lowest permeation rate and its water flux hardly varied with the pressure; thus, a rigid behavior of the chitosan chains under the pressure action can be presumed. As result of a barrier formation on the crosslinked surface, the enhanced network hinders the water transport across the film. However, this reduction of water flux, as compared with pure chitosan and homogeneous crosslinking samples, could be a promising factor to improve the rejection selectivity of chitosan membranes, since a tailored free volume reduction could restrict the diffusion of specific molecules into the membrane according to its size and charge [31,45].

The estimated permeability of the prepared films is recorded in Table 6. It should be emphasized that the linear performance of water permeation disappeared at high values of applied pressure for CS membrane (Δp > 10 bar, Fig. 4). Thus, the permeability was determined by considering only water flux values included within the linear interval.

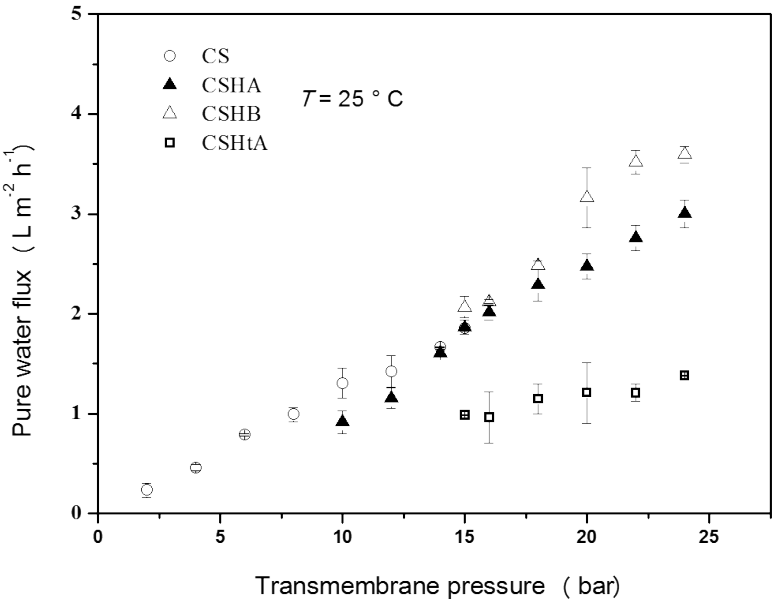

Fig. 4. Evolution of water flux for prepared films as function of pressure.

3.3.2 Aqueous Cu^{2+} permeation experiments

The fouling performance and rejection potential of neat and crosslinking chitosan membranes were characterized with a divalent salt aqueous solution ($CuSO_4$). The salt rejection performance of membranes is an important factor for many industrial applications, especially involving separation of mono/divalent salts from small molecular weight organics [19]. Besides the mutual affinity of membrane and solute, other factors could affect the salt rejection potential such as membrane porosity. The transport mechanism determining the rejection performance of non-porous membranes is described in the literature by the well-known solution diffusion model [45,46]. Waheed et al. explained that solute transport within the membranes involves three steps: 1) sorption at the surface of the membrane, 2) diffusion into dense membrane under pressure, and 3) solute desorption [47].

Fig. 5A shows the temporal evolution of the permeate flux for copper sulfate solutions. Crosslinking membranes exhibited steady fluxes with time, whereas for the neat CS membrane a gradual flux decline was observed throughout the experiment. This behavior could be attributed to the non-stable mechanical evolution of chitosan film that shrinks under continuously applied pressure as mentioned above.

In order to evaluate the fouling extent promoted by the salt interaction with the membranes matrix, two parameters were analyzed: relative flux (*RF*), obtained with Eq. 8, and flux recovery rate (*FRR*) calculated as the pure water fluxes ratio before and after the copper(II) filtration experiments (J_{wf}/J_{wi} values in Table 6). All flux parameters were calculated with the values obtained at the end of each experiment.

Table 6. Water flux performance and Cu^{2+} filtration on chitosan membranes.

Membrane	**Permeability** (L m^{-2} h^{-1} bar^{-1})	$J_{Cu^{2+}}/J_{water}$ (Δp = 15 bar; T = 25 ºC)	J_{wf}/J_{wi}
CS neat	0.12	0.62	1.00
CSHA	0.13	0.97	0.98
CSHtA	0.04	1.00	1.00

From $J_{Cu^{2+}}/J_{water}$ data summarized in Table 6 is apparent that the permeation rate of crosslinking membranes is not affected by the presence of $CuSO_4$ in the feed solution. Thus,

the flows of salt solutions slightly decreased or were similar to the pure water flux. This fact could be explained by the capacity of the crosslinking membranes to maintain the mechanical stability under pressure, which provided no changes in the structure of the membranes allowing the water flow, while retaining the metal ions as mentioned below.

However, solution flux of the neat CS membrane decreased with filtration time. This effect could be ascribed to both a further compaction of chitosan structure and the deposition/adsorption of metal ions onto the membrane surface and into the inner structure of membrane. Interactions between metal ions and amino groups could reduce the flexibility and mobility of chitosan chains and thus lowering the flow through the membrane.

The flux recovery was explored comparing the water flux after membrane cleaning (J_{wf}) and the initial flux (J_{wi}) before salt filtration. Membranes were cleaned with deionized water at zero transmembrane pressure during 1 h. The results suggest that the prepared membranes can be reused after filtration of copper solutions considering that J_{wf}/J_{wi} values are practically equal to unity; hence, the membrane fouling should be considered as reversible taking into account that is possible to restore the initial permeate flux after physical cleaning. Therefore, the use of chitosan membranes could be a viable and economic approach for the wastewater treatment.

Figure 5B shows the temporal evolution of copper concentration in feed and permeate streams with the filtration time. The copper transport is almost constant for all of tested membranes during the permeation time (6 h). The variation of copper content in the feed streams is insignificant during the filtration of salt solution. It is evident that copper content collected in the permeate stream for neat CS membrane is higher than the solute permeation observed for the crosslinking membranes. The ion transport grade for neat chitosan membrane can be influenced by the water permeation rate and by the copper diffusion in agreement with concentration profile formed through the membrane cross-section.

It can be worthy to compare the results of static adsorption with filtration experiments, since a preferential solute sorption on the surface films could promote the ions diffusion into the dense membrane and the corresponding transport to the permeate side under external pressure. This correlation was found when comparing the copper adsorption and filtration performances of neat chitosan and heterogeneous crosslinked membranes. Thus, copper ions

transport through CS films was favored by the initial sorption on the chitosan surface; conversely, the deficient adsorption of Cu^{2+} ions on the surface of CHtA and CHtB samples prevented their further diffusion across the films during filtration experiments. However, the most streaking behavior was found for the homogenously crosslinked membranes, where the intense surface adsorption (similar to the neat chitosan specimen) yielded no appreciable copper flow across the membranes. The blockage of the internal amino groups by the crosslinking agent (sulfuric acid) could explain this effect due to the reduction of available sites with chemical affinity to the diffusing Cu^{2+} ions.

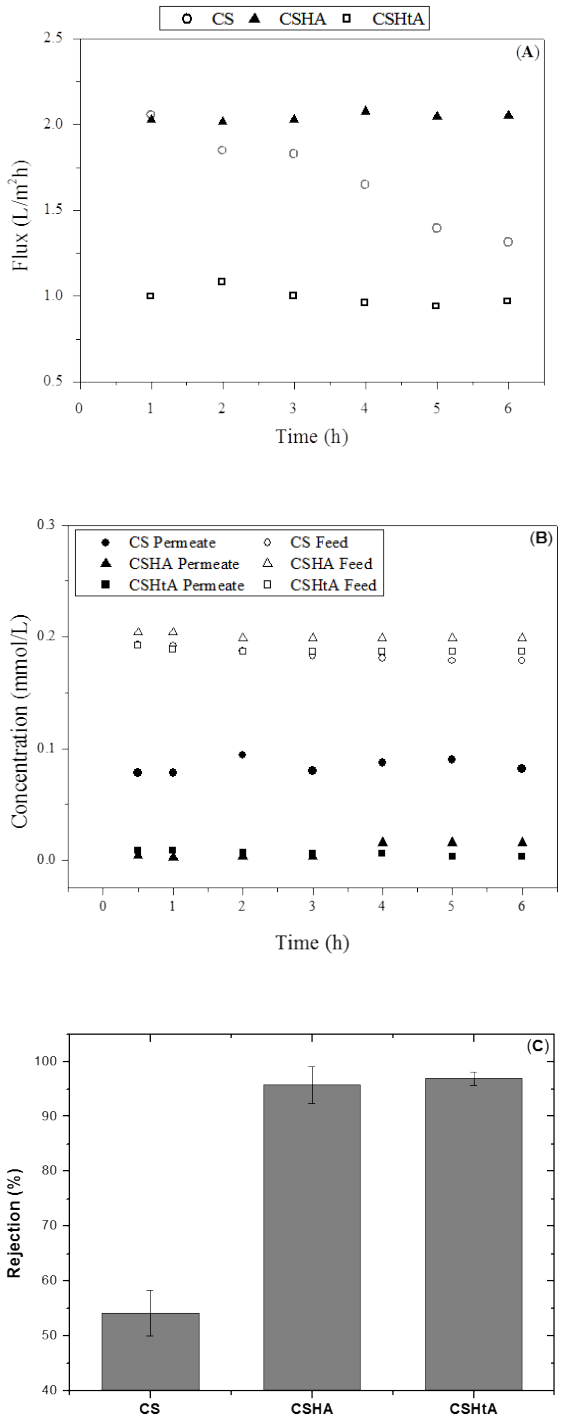

Fig. 5. Membrane permeation performance for Cu^{2+}solutions (14 ppm, Δp = 15 bar; T = 25 ºC).

(A) Temporal evolution of permeate flux.

(B) Temporal evolution of copper concentration.

(C) Membrane rejection.

At last, the rejection potential of CS, CSHtA, and CSHA membranes, calculated by Eq. 7 from the metal concentration in the permeate and feed streams, was displayed in Fig. 5C. As seen in the figure, both crosslinking membranes, CSHA and CSHtA, exhibited an excellent rejection potential that improved the performance of the neat CS sample around a 40%. However, it was apparent that the CSHA film achieved this remarkable rejection while preserving a relevant permeate flux in contrast with CSHtA membrane (Figure 5A). Therefore, since the initial water flux value is quite similar to the final one, and considering the stable (temporally) performance of salt membrane permeation observed, neither pore blocking nor cake filtration can be considered as feasible descriptors to analyze the possible membrane fouling mechanisms.

Accordingly, the improved metal rejection, enhanced mechanical properties, adequate and constant flux during filtration experiments, along with suitable antifouling behavior, reveal that the homogeneous crosslinking chitosan membranes prepared in this investigation can be considered as promising filtration materials to be applied in future applications concerning water treatment.

4. Conclusions

In this study, the performances for aqueous Cu^{2+} adsorption and filtration were evaluated for chitosan and four different chitosan-based films obtained by crosslinking with sulfuric acid. Two manufacture procedures were essayed, homogeneous crosslinking (one-step synthesis) and heterogeneous crosslinking (immersion of chitosan films in acidic medium).

The adsorption of aqueous Cu^{2+} on the films surface was characterized through kinetic and equilibrium experiments. Neat chitosan (CS) and homogeneous crosslinking samples (CSHA, CSHB) exhibited a rather similar behavior, whereas heterogeneous crosslinking films (CSHtA, CSHtB) showed a poorer copper adsorption. Adsorption saturation of the films was observed in no case and the Freundlich model was thoroughly preferable. The kinetic study revealed that the pseudo-second order equation was adequate to reproduce the temporal evolution of the Cu(II) adsorption.

Chitosan and cross-linked chitosan films behaved as dense membranes in the course of the filtration essays. Pure water permeability was systematically found low, especially for

the heterogeneous samples. The flux temporal evolution observed for cross-linked membranes during Cu(II) solutions filtration was stable, although the value found for the homogeneous sample was significantly higher. Conversely, the solution flux of the neat chitosan membrane declined around 40% after six hours showing that the structural stability of pure chitosan films was inadequate for water treatment purpose.

All the prepared membranes exhibited excellent antifouling properties during copper filtration experiments. In addition, both cross-linked processes enhanced the Cu^{2+} rejection in a similar extent, around 40%. Consequently, it was possible to conclude that the homogeneously cross-linked film CSHA appeared as a promising material for adsorption and rejection of aqueous copper solutions by combining improved metal rejection, enhanced mechanical resistance, adequate and constant flux, and suitable antifouling behavior during filtration experiments.

Acknowledgments

Financial support for this work was provided by the Ministerio de Economía y Competitividad through the research project CTM2015-69246-R (MINECO/FEDER, UE). The authors also would like to thank the Chemical Institute of Federal University of Rio Grande do Norte. The scholarship for J.S. Marques from CAPES (Coordenação de Aperfeiçoamento de Pessoal de Nível Superior) and PRHPB22 (Programa Petrobrás de Recursos Humanos) is also gratefully acknowledged.

Data availability

The raw/processed data required to reproduce these findings cannot be shared at this time due to technical or time limitations.

References

[1] B. Krajewska, Diffusion of metal ions through gel chitosan membranes, React. Funct. Polym. 47 (2001) 37–47. doi:10.1016/S1381-5148(00)00068-7.

[2] K. V. Harish Prashanth, R.N. Tharanathan, Chitin/chitosan: modifications and their unlimited application potential-an overview, Trends Food Sci. Technol. 18 (2007) 117–131. doi:10.1016/j.tifs.2006.10.022.

[3] C.K.S. Pillai, W. Paul, C.P. Sharma, Chitin and chitosan polymers: Chemistry, solubility and fiber formation, Prog. Polym. Sci. 34 (2009) 641–678. doi:10.1016/j.progpolymsci.2009.04.001.

[4] G.C. Steenkamp, K. Keizer, H.W.J.P. Neomagus, H.M. Krieg, Copper (II) removal from polluted water with alumina / chitosan composite membranes, J. Memb. Sci. 197 (2002) 147–156. doi:https://doi.org/10.1016/S0376-7388(01)00608-1.

[5] M. Dash, F. Chiellini, R.M. Ottenbrite, E. Chiellini, Chitosan - A versatile semi-synthetic polymer in biomedical applications, Prog. Polym. Sci. 36 (2011) 981–1014. doi:10.1016/j.progpolymsci.2011.02.001.

[6] B. Liu, D. Wang, G. Yu, X. Meng, Adsorption of heavy metal ions, dyes and proteins by chitosan composites and derivatives - A review, J. Ocean Univ. China. 12 (2013) 500–508. doi:10.1007/s11802-013-2113-0.

[7] R.S. Vieira, M.L.M. Oliveira, E. Guibal, E. Rodríguez-Castellón, M.M. Beppu, Copper, mercury and chromium adsorption on natural and crosslinked chitosan films: An XPS investigation of mechanism, Colloids Surfaces A Physicochem. Eng. Asp. 374 (2011) 108–114. doi:10.1016/j.colsurfa.2010.11.022.

[8] P. Baroni, R.S. Vieira, E. Meneghetti, M.G.C. da Silva, M.M. Beppu, Evaluation of batch adsorption of chromium ions on natural and crosslinked chitosan membranes, J. Hazard. Mater. 152 (2008) 1155–1163. doi:10.1016/j.jhazmat.2007.07.099.

[9] S.G. Caridade, R.M.P. da Silva, R.L. Reis, J.F. Mano, Effect of solvent-dependent viscoelastic properties of chitosan membranes on the permeation of 2-phenylethanol, Carbohydr. Polym. 75 (2009) 651–659. doi:10.1016/j.carbpol.2008.09.011.

[10] S.S. Shenvi, S.A. Rashid, A.F. Ismail, M.A. Kassim, A.M. Isloor, Preparation and characterization of PPEES/chitosan composite nanofiltration membrane, Desalination. 315 (2013) 135–141. doi:10.1016/j.desal.2012.09.009.

[11] A.G. Karakeçili, C. Satriano, M. Gümüşderelioğlu, G. Marletta, Surface characteristics of ionically crosslinked chitosan membranes, J. Appl. Polym. Sci. 106 (2007) 3884–3888. doi:10.1002/app.26920.

[12] A. de A. Gonsalves;, C.R.M. Araújo;, N.A. Soares;, M.O.F. Goulart;, F.C. de Abreu, Diferentes estratégias para a reticulação de quitosana, Quim. Nova. 34 (2011) 1215–1223. doi:http://dx.doi.org/10.1590/S0100-40422011000700021.

[13] J.S. Marques, J.A.O.D. Chagas, J.L.C. Fonseca, M.R. Pereira, Comparing homogeneous and heterogeneous routes for ionic crosslinking of chitosan membranes, React. Funct. Polym.

103 (2016) 156–161. doi:10.1016/j.reactfunctpolym.2016.04.014.

[14] R. Rabelo, R. Vieira, F. Luna, E. Guibal, M. Beppu, Adsorption of Copper(II) and Mercury(II) Ions onto Chemically-modified Chitosan Membranes: Equilibrium and Kinetic Properties, Adsorpt. Sci. Technol. 30 (2012) 1–22. doi:10.1260/0263-6174.30.1.1.

[15] N.M. Alves, J.F. Mano, Chitosan derivatives obtained by chemical modifications for biomedical and environmental applications, Int. J. Biol. Macromol. 43 (2008) 401–414. doi:10.1016/j.ijbiomac.2008.09.007.

[16] F.-C. Wu, R.-L. Tseng, R.-S. Juang, A review and experimental verification of using chitosan and its derivatives as adsorbents for selected heavy metals., J. Environ. Manage. 91 (2010) 798–806. doi:10.1016/j.jenvman.2009.10.018.

[17] J. Ge, Y. Cui, Y. Yan, W. Jiang, The effect of structure on pervaporation of chitosan membrane, J. Memb. Sci. 165 (2000) 75–81. doi:10.1016/S0376-7388(99)00228-8.

[18] C.K. Yeom, S.H. Lee, J.M. Lee, Effect of the ionic characteristics of charged membranes on the permeation of anionic solutes in reverse osmosis, J. Memb. Sci. 169 (2000) 237–247. doi:10.1016/S0376-7388(99)00341-5.

[19] D. a Musale, A. Kumar, Effects of surface crosslinking on sieving characteristics of chitosan/poly(acrylonitrile) composite nanofiltration membranes, Sep. Purif. Technol. 21 (2000) 27–37. doi:10.1016/S1383-5866(00)00188-X.

[20] M.M. Beppu, R.S. Vieira, C.G. Aimoli, C.C. Santana, Crosslinking of chitosan membranes using glutaraldehyde: Effect on ion permeability and water absorption, J. Memb. Sci. 301 (2007) 126–130. doi:10.1016/j.memsci.2007.06.015.

[21] J.N. Shen, C.C. Yu, G.N. Zeng, B. van der Bruggen, Preparation of a facilitated transport membrane composed of carboxymethyl chitosan and polyethylenimine for CO2/N2 separation, Int. J. Mol. Sci. 14 (2013) 3621–3638. doi:10.3390/ijms14023621.

[22] M.R. Pereira, J.S. Marques, J.L.C. Fonseca, Biocomposites based on chitosan and carnauba straw powder, Polímeros Ciência E Tecnol. 24 (2014) 446–452. doi:10.1590/0104-1428.1551.

[23] J.M. Arsuaga, M.J. López-Muñoz, A. Sotto, Correlation between retention and adsorption of phenolic compounds in nanofiltration membranes, Desalination. 250 (2010) 829–832. doi:10.1016/j.desal.2008.11.051.

[24] Z. Cheng, X. Liu, M. Han, W. Ma, Adsorption kinetic character of copper ions onto a modified chitosan transparent thin membrane from aqueous solution, J. Hazard. Mater. 182 (2010) 408–415. doi:10.1016/j.jhazmat.2010.06.048.

[25] A.L.P.F. Caroni, C.R.M. de Lima, M.R. Pereira, J.L.C. Fonseca, Tetracycline adsorption on chitosan: A mechanistic description based on mass uptake and zeta potential measurements, Colloids Surfaces B Biointerfaces. 100 (2012) 222–228. doi:10.1016/j.colsurfb.2012.05.024.

[26] R. Laus, T.G. Costa, B. Szpoganicz, V.T. Fávere, Adsorption and desorption of Cu(II), Cd(II) and Pb(II) ions using chitosan crosslinked with epichlorohydrin-triphosphate as the

adsorbent, J. Hazard. Mater. 183 (2010) 233–241. doi:10.1016/j.jhazmat.2010.07.016.

[27] M.J. López-Muñoz, A. Sotto, J.M. Arsuaga, B. Van der Bruggen, Influence of membrane, solute and solution properties on the retention of phenolic compounds in aqueous solution by nanofiltration membranes, Sep. Purif. Technol. 66 (2009) 194–201. doi:10.1016/j.seppur.2008.11.001.

[28] S. Rivero, M.A. García, A. Pinotti, Crosslinking capacity of tannic acid in plasticized chitosan films, Carbohydr. Polym. 82 (2010) 270–276. doi:10.1016/j.carbpol.2010.04.048.

[29] Z. Cui, Y. Xiang, J. Si, M. Yang, Q. Zhang, T. Zhang, Ionic interactions between sulfuric acid and chitosan membranes, Carbohydr. Polym. 73 (2008) 111–116. doi:10.1016/j.carbpol.2007.11.009.

[30] A.L.P.F. Caroni, C.R.M. de Lima, M.R. Pereira, J.L.C. Fonseca, The kinetics of adsorption of tetracycline on chitosan particles, J. Colloid Interface Sci. 340 (2009) 182–191. doi:10.1016/j.jcis.2009.08.016.

[31] R.Y.M. Huang, R. Pal, G.Y. Moon, Crosslinked chitosan composite membrane for the pervaporation dehydration of alcohol mixtures and enhancement of structural stability of chitosan/polysulfone composite membranes, J. Memb. Sci. 160 (1999) 17–30. doi:10.1016/S0376-7388(99)00074-5.

[32] W. Won, X. Feng, D. Lawless, Separation of dimethyl carbonate/methanol/water mixtures by pervaporation using crosslinked chitosan membranes, Sep. Purif. Technol. 31 (2003) 129–140. doi:10.1016/S1383-5866(02)00176-4.

[33] H.S. Tsai, Y.Z. Wang, Properties of hydrophilic chitosan network membranes by introducing binary crosslink agents, Polym. Bull. 60 (2008) 103–113. doi:10.1007/s00289-007-0846-x.

[34] L. Mengatto, M.G. Ferreyra, A. Rubiolo, I. Rintoul, J. Luna, Hydrophilic and hydrophobic interactions in cross-linked chitosan membranes, Mater. Chem. Phys. 139 (2013) 181–186. doi:10.1016/j.matchemphys.2013.01.019.

[35] M. Kumar, B.P. Tripathi, V.K. Shahi, Crosslinked chitosan/polyvinyl alcohol blend beads for removal and recovery of Cd(II) from wastewater, J. Hazard. Mater. 172 (2009) 1041–1048. doi:10.1016/j.jhazmat.2009.07.108.

[36] A. Domard, pH and c.d. measurements on a fully deacetylated chitosan: application to CuII-polymer interactions, Int. J. Biol. Macromol. 9 (1987) 98–104. doi:10.1016/0141-8130(87)90033-X.

[37] A. Ghaee, M. Shariaty-Niassar, J. Barzin, T. Matsuura, Effects of chitosan membrane morphology on copper ion adsorption, Chem. Eng. J. 165 (2010) 46–55. doi:10.1016/j.cej.2010.08.051.

[38] N. Li, R. Bai, Copper adsorption on chitosan-cellulose hydrogel beads: Behaviors and mechanisms, Sep. Purif. Technol. 42 (2005) 237–247. doi:10.1016/j.seppur.2004.08.002.

[39] E. Guibal, Interactions of metal ions with chitosan-based sorbents: A review, Sep. Purif. Technol. 38 (2004) 43–74. doi:10.1016/j.seppur.2003.10.004.

[40] F. Zhao, E. Repo, D. Yin, M.E.T. Sillanpää, Adsorption of Cd (II) and Pb (II) by a novel EGTA-modified chitosan material : Kinetics and isotherms, J. Colloid Interface Sci. 409 (2013) 174–182. doi:10.1016/j.jcis.2013.07.062.

[41] C. Gerente, V.K.C. Lee, P. Le Cloirec, G. McKay, Application of Chitosan for the Removal of Metals From Wastewaters by Adsorption—Mechanisms and Models Review, Crit. Rev. Environ. Sci. Technol. 37 (2007) 41–127. doi:10.1080/10643380600729089.

[42] E.C.N. Lopes, F.S.C. dos Anjos, E.F.S. Vieira, A.R. Cestari, An alternative Avrami equation to evaluate kinetic parameters of the interaction of Hg(II) with thin chitosan membranes, J. Colloid Interface Sci. 263 (2003) 542–547. doi:10.1016/S0021-9797(03)00326-6.

[43] D. Baskar, T.S. Sampath Kumar, Effect of deacetylation time on the preparation, properties and swelling behavior of chitosan films, Carbohydr. Polym. 78 (2009) 767–772. doi:10.1016/j.carbpol.2009.06.013.

[44] M. Pieróg, M. Gierszewska-Dróżyńska, J. Ostrowska-Czubenko, Effect of ionic crosslinking agents on swelling behavior of chitosan hydrogel membranes, Prog. Chem. Appl. Chitin Its.. XIV (2009) 75–82. http://www.ptchit.lodz.pl/file-PTChit_(mek53429puet47b3).pdf.

[45] E. Salehi, S.S. Madaeni, L. Rajabi, A.A. Derakhshan, S. Daraei, V. Vatanpour, Static and dynamic adsorption of copper ions on chitosan/polyvinyl alcohol thin adsorptive membranes: Combined effect of polyethylene glycol and aminated multi-walled carbon nanotubes, Chem. Eng. J. 215–216 (2013) 791–801. doi:10.1016/j.cej.2012.11.071.

[46] T. Bellincanta, P. Poletto, M.B. Thürmer, J. Duarte, A. Toscan, M. Zeni, Preparação e Caracterização de Membranas Poliméricas a partir da Blenda Polisulfona / Poliuretano, 21 (2011) 229–232. doi:10.1590/S0104-14282011005000045.

[47] S. Waheed, A. Ahmad, S.M. Khan, S. e. Gul, T. Jamil, A. Islam, T. Hussain, Synthesis, characterization, permeation and antibacterial properties of cellulose acetate/polyethylene glycol membranes modified with chitosan, Desalination. 351 (2014) 59–69. doi:10.1016/j.desal.2014.07.019.

Tables

Table 1.
Membrane casting solution composition.

Membrane	Ratio SO_4^{2-}/NH_3^+	Immersion time (min)	Contact angle (°)
CS	-	-	88.2
CSHA	1 : 6	-	88.6
CSHB	1 : 4	-	90.3
CSHtA	-	5	96.4
CSHtB	-	30	95.1

Table 2.
Removal of aqueous Cu^{2+} attained with the prepared membranes after contact during 48 h.

Membrane	Percent removal (%)		
	14 ppm (30 °C)	100 ppm (30°C)	100 ppm (15 °C)
CS	73	42	46
CSHA	80	53	59
CSHB	73	54	38
CSHtA	14	22	9
CSHtB	13	2	4

Table 3.
Kinetics parameters for the adsorption of Cu^{2+} ions on chitosan membranes.

		Pseudo-first order			***Pseudo-second order***		
		q_e (mmol m^2)	k_1 (h^{-1})	R^2	q_e (mmol m^2)	k_2 (h^{-1})	R^2
Adsorption of Cu^{2+} ions at 30 °C (14 ppm)	CS	12.0	0.123	0.937	12.8	0.017	0.994
	CSHA	10.1	0.109	0.961	11.0	0.015	0.989
	CSHB	12.0	0.097	0.986	12.4	0.023	0.991
	CSHtA	2.5	0.109	0.310	2.59	0.336	0.974
	CSHtB	2.7	0.114	0.795	4.04	0.013	0.887
Adsorption of Cu^{2+} ions at 30 °C (100 ppm)	CS	51.7	0.139	0.983	53.5	0.010	0.999
	CSHA	64.5	0.134	0.978	69.4	0.004	0.992
	CSHB	65.5	0.125	0.922	69.9	0.003	0.985
	CSHtA	28.0	0.108	0.973	32.5	0.004	0.904
	CSHtB	7.2	0.0.4	0.148	5.81	0.666	0.999
Adsorption of Cu^{2+} ions at 15 °C (100 ppm)	CS	50.0	0.145	0.868	53.1	0.009	0.981
	CSHA	58.0	0.079	0.969	62.6	0.002	0.989
	CSHB	43.5	0.090	0.994	51.3	0.002	0.976
	CSHtA	12.9	0.106	0.737	12.8	0.256	0.999
	CSHtB	5.5	0.0093	0.416	5.40	0.249	0.998

Table 4.
Parameters kinetics of intra-particle diffusion model for the adsorption of Cu^{2+} ions on chitosan membranes.

Membrane	Adsorption Cu^{2+} ions					
	14 ppm (30°C)		100 ppm (30°C)		100 ppm (15°C)	
	k_{id}	R^2	k_{id}	R^2	k_{id}	R^2
CS	1.62	0.899	5.56	0.837	6.61	0.903
CSHA	1.45	0.954	8.63	0.942	11.35	0.916
CSHB	1.42	0.946	8.76	0.972	10.69	0.908
CSHtA	0.35	0.443	4.16	0.872	0.525	0.684
CSHtB	0.49	0.877	0.41	0.238	0.362	0.611

Table 5. Adsorption isotherm parameters for adsorption of Cu^{2+} ions by chitosan membranes.

	Langmuir			Freundlich		
	Q_{max} (mmol m^2)	b	R^2	k_F	n	R^2
CS neat	179	0.277	0.894	31.7	0.79	0.988
CSHA	172	0.233	0.867	28.1	0.85	0.986
CSHB	147	0.687	0.983	41.8	1.43	0.911
CSHtA	47	0.310	0.243	8.77	0.41	0.537
CSHtB	39	0.481	0.299	9.72	0.34	0.673

Table 6. Water flux performance and Cu^{2+} filtration on chitosan membranes.

Membrane	Permeability (L m^{-2} h^{-1} bar^{-1})	$J_{Cu^{2+}}/J_{water}$	RF, J_{wf}/J_{wi}
CS neat	0.12	0.62	1.00
CSHA	0.13	0.99	0.98
CSHtA	0.04	1.00	1.00

Supplementary Information

FIGURES

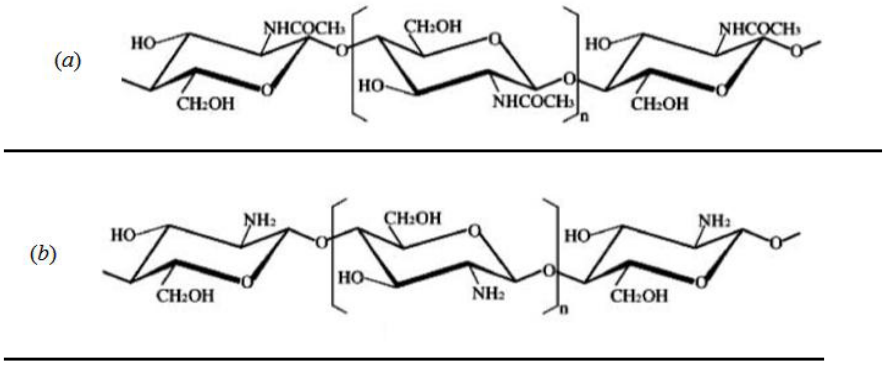

Fig. 1S. Comparison between chitin (a) and chitosan (b).

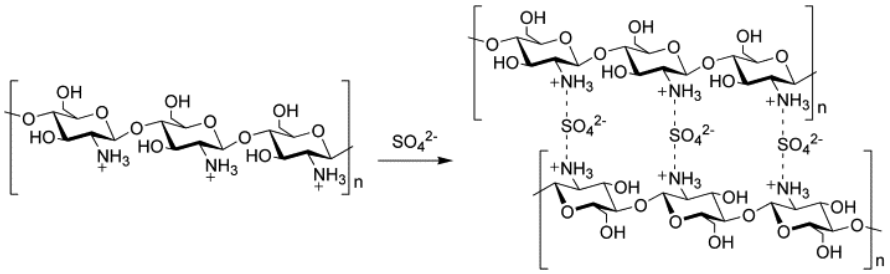

Fig. 2S. Ionic crosslinking with sulfuric acid of chitosan films as proposed by Cui et al. [29].

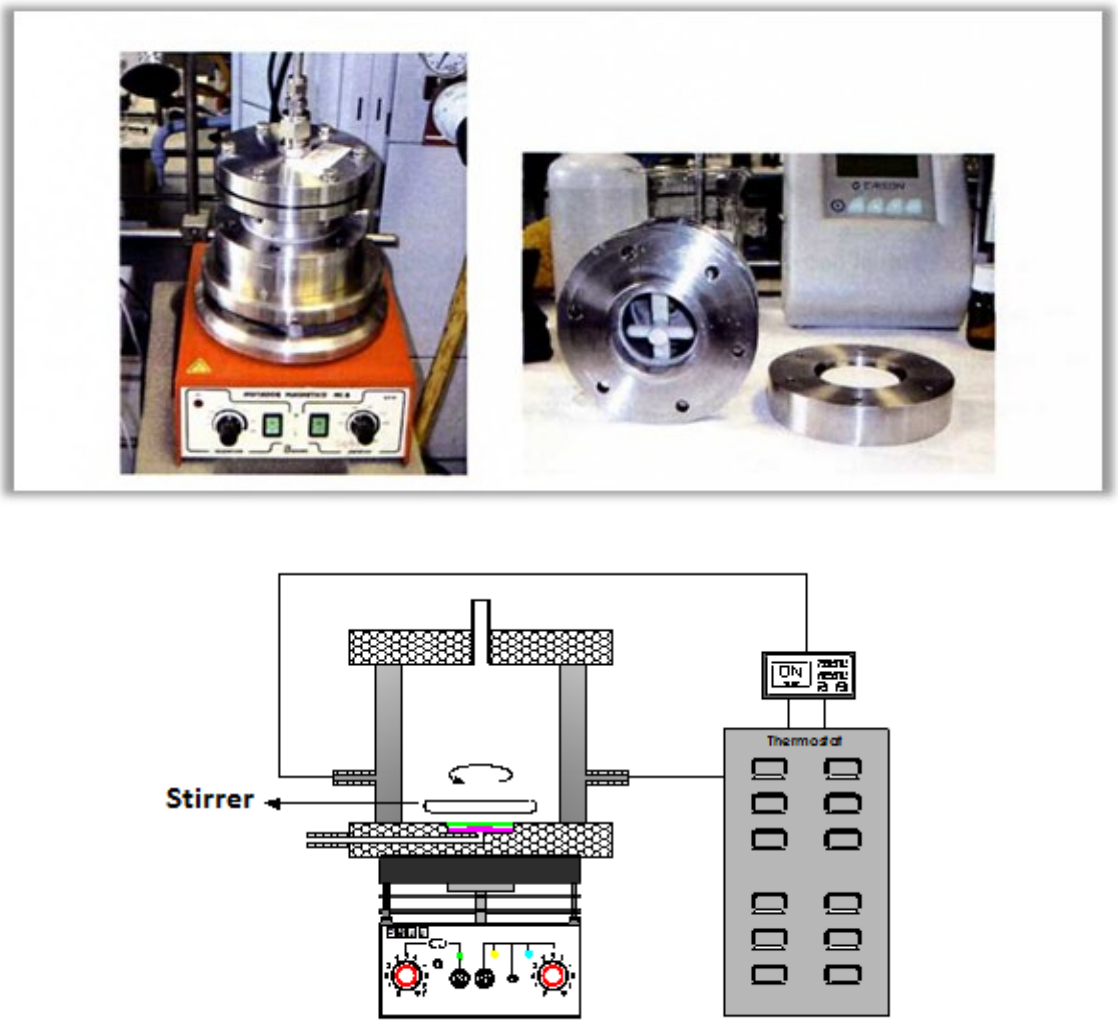

Fig. 3S. Experimental equipment (photographs and scheme) for the determination of aqueous Cu(II) adsorption on chitosan films.

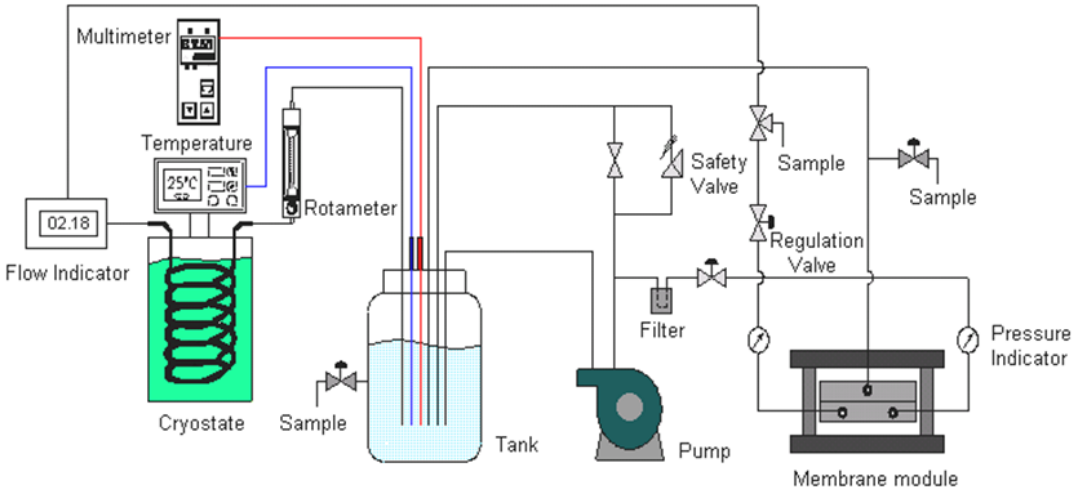

Fig. 4S. Experimental equipment for the determination of the filtration performance of pure and crosslinked chitosan films.

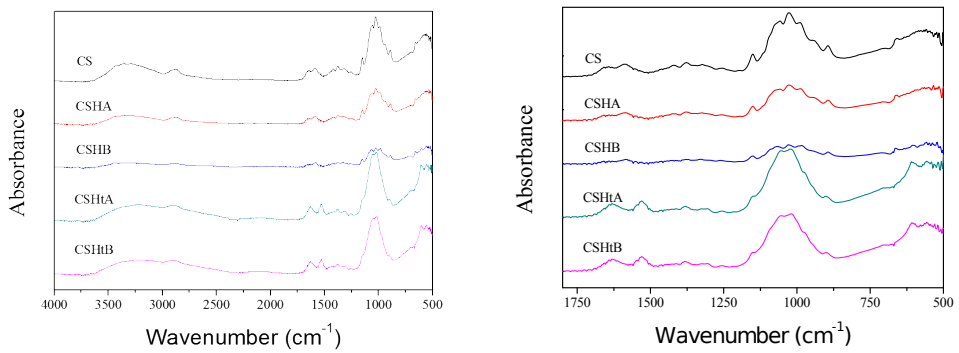

Fig. 5S. FTIR-ATR spectra of manufactured chitosan membranes.

Comment: The crosslinking process of chitosan with sulfuric acid occurred through the electrostatic interactions between the protonated amino groups (NH_3^+) and the SO_4^{2-} ions [29]. The vanishing of bands corresponding to amino groups (amide I band at 1645 cm^{-1} and amide II band at 1580 cm^{-1}) and the appearance of two news bands at 1630 cm^{-1} and 1530 cm^{-1} confirmed the expected chemical reaction. Fig. 2S reveals that, as result of the heterogeneously crosslinking process, the chemical structure of films was more significantly changed in comparison with the effect observed for the homogeneously crosslinked samples. Actually, the FTIR-ATR spectra of CSH samples were quite similar to the neat chitosan one. This fact can be attributed to the lower ratio of crosslinking agent required to prepare the CSH films that, however, was adequate to prevent the solubility of material in acidic media.

TABLES

Table 1S.
Thickness of the prepared films (adapted from Marques *et al.* [13]).

Sample	Thickness (mm)
CS	0.05 ± 0.01
CSHA	0.05 ± 0.01
CSHB	0.06 ± 0.01
CSHtA	0.07 ± 0.01
CSHtB	0.07 ± 0.01

Table 2S.
Experimental Cu(II) adsorption at 48 h, q_e(exp), for the prepared chitosan films.

		q_e**(exp)** (mmol m^2)
Adsorption of Cu^{2+} ions at 30 °C (14 ppm)	CS neat	12.0
	CSHA	10.0
	CSHB	11.1
	CSHtA	2.5
	CSHtB	2.6
Adsorption of Cu^{2+} ions at 30 °C (100 ppm)	CS neat	51.7
	CSHA	64.4
	CSHB	65.4
	CSHtA	27.9
	CSHtB	5.8
Adsorption of Cu^{2+} ions at 15 °C (100 ppm)	CS neat	52.0
	CSHA	58.3
	CSHB	42.9
	CSHtA	12.7
	CSHtB	5.3